applied sciences

MDPI

Article

A Systematic Approach of Optimal Land-Use Planning by Applying Geo-Environmental Techniques: A Case Study

Essam A. Morsy [1,2]

[1] Department of Environmental and Health Research, Umm Al-Qura University, P.O. Box 6287, Makkah 21955, Saudi Arabia; eamibrahim@uqu.edu.sa
[2] Geophysics Department, Faculty of Science, Cairo University, Giza P.O. Box 12613, Egypt

Abstract: This article demonstrates the capabilities and integrity of the environmental geological and geophysical techniques for planning the suitability of the extension of Helwan city for construction and engineering purposes. The geological and topographical mapping were utilized as well as environmental geophysical techniques (seismic refraction, ground penetrating radar (GPR), and resistivity soundings) for optimal land-use planning. The seismic refraction profiles were conducted to evaluate the geotechnical characteristics of the bedrock, GPR was applied to define the main subsurface reflectors, and the geoelectrical resistivity survey was used to identify the subsurface stratigraphic sequence and the distribution of main structural elements impacting the investigated area. The integrated results and findings of the environmental geological and geophysical survey inferred two major distinctive subsurface layers: a thin surface layer represented by highly weathered limestone, with an average thickness of 3 m, and a bottom layer equivalent to the bedrock composed of hard limestone. In addition, GPR performed an analysis of two remarkable subsurface layers, which supported the generated model of other geophysical surveying techniques. Finally, all the geological and various geophysical techniques were integrated and merged to generate the optimal land-use plan of the extension of Helwan city for construction and engineering purposes and to avoid high-risk areas to reserve the sustainability of the new urban communities.

Keywords: integrity; environmental; geological; geophysical; sustainability

check for updates

Citation: Morsy, E.A. A Systematic Approach of Optimal Land-Use Planning by Applying Geo-Environmental Techniques: A Case Study. *Appl. Sci.* **2023**, *13*, 1749. https://doi.org/10.3390/app13031749

Academic Editor: Jianbo Gao

Received: 17 November 2022
Revised: 15 January 2023
Accepted: 27 January 2023
Published: 30 January 2023

Copyright: © 2023 by the author. Licensee MDPI, Basel, Switzerland. This article is an open access article distributed under the terms and conditions of the Creative Commons Attribution (CC BY) license (https://creativecommons.org/licenses/by/4.0/).

1. Introduction

As populations grow, available land will become a scarce natural resource, especially for the already-existing urban communities. As more land is planned to be developed, effective planning will counteract the negative effects of its use and development. The numerous benefits of effective land-use planning can include the following: creating a generic framework for the proposed urban project, aiding the anticipation of the future plan of the investigated site, implementing sustainable infrastructure utilities, direct positive impact on the local urban economy, optimal use and conservation of natural resources along with protection of the environment, minimizing the associated risks of the natural hazards, and avoiding land-use conflicts [1–3].

For an optimal planning and effective development of the investigated site, a suggested joint integrated approach of geophysical methods including the electrical resistivity, seismic refraction methods, ground penetrating radar, and geological mapping were implemented throughout the study area. Geophysical indicators, including electrical resistivity, seismic velocity, and electromagnetic signature, give a clear image about the subsurface layering sequence and the degree of rock weathering or fracturing [4,5].

The investigated site is situated at the southeastern sector of Cairo, Egypt, which was designated for a proposed residential extension of the already-existing Helwan city, to reduce/minimize the random distribution of the unplanned urbanization in addition to providing millions of job opportunities, which takes into account the provision of a

better life to the citizen through housing, investment, and work opportunities, and makes unremitting efforts to confront unplanned or random real estate growth [6,7].

Climatically, Helwan city is characterized by a hot and humid climate, as temperatures rise during the summer to reach 39 °C in June, with its lowest extent of 19 °C during January. The average humidity ranges between 60% to 90%. As for rain, it is relatively little and mostly falls during the winter season [8,9].

Sharp land cover changes have been caused due to tremendous increases in urbanization and industry over the Greater Cairo Region (GCR), Egypt. Urban variation was observed during the last two decades, as shown in Figure 1, with the rate of urbanization during the last two decades (1999, 2011, and 2016) increasing rapidly, which calls for optimal urban planning in that area [10].

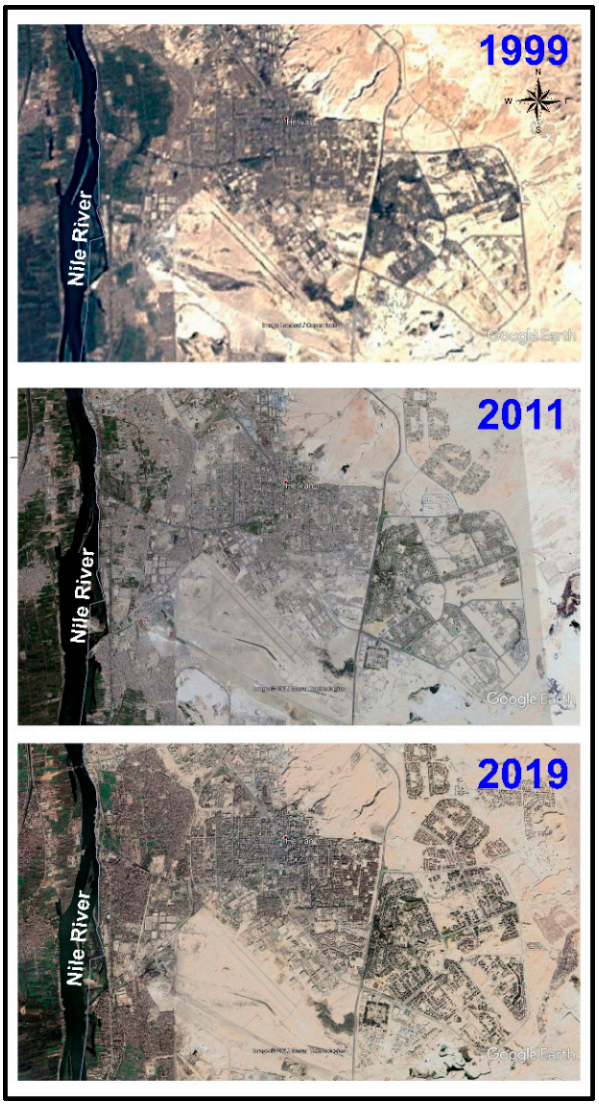


Figure 1. Comparison of the urbanization pattern during 1999, 2011, and 2019 on Helwan City.

Geologically, the investigated site is bordered to the east and north as well as to the northwest by known geological plateaus, such as the observatory plateau that bounds the studied area from the northwest, and the Qurn Plateau that borders the study area from the east, in addition to the Halawan highlands that are located southeast of the study area [11–13]. These plateaus can be described as the following: (1) an observatory plateau that varies from 117–150 m, which descends a very simple slope towards the south and southwest and consists of limestone rocks and dolomitic limestone of the upper part of the

Middle Eocene, as illustrated in Figure 2, and which is outcropped by quarrying activities northwest and southwest of the investigated site and diminishes gradually to the west and southwest of the investigated site; (2) the Qurn Plateau of an elevation that ranges from 117–215 m, characterized by a longitudinal rocky elevation, which is located directly above the observatory plateau and consists of limestone and marly limestone belonging to Upper Eocene; and (3) Helwana Heights of an elevation ranging from 239–1002 m, located southeast of the investigated site and also extending from the Qurn Plateau, separated by Harbu Valley.

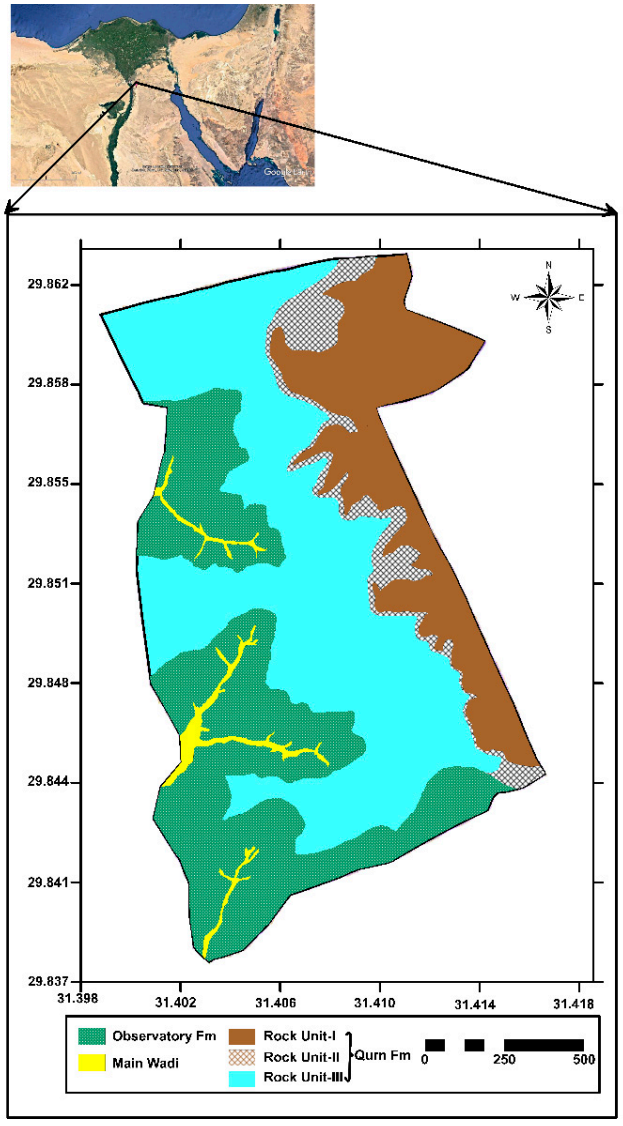


Figure 2. A map showing the geological units of the investigated site with respect to Egypt.

Topographically, the geological setting of the investigated site directly impacted the topographical regime, as they are inter-related, where the general topographical regime (high plateaus and terraces) is influenced completely by weathering and erosion processes. The range of elevations through the study area is between 155–233 m, and most parts of the study area were formed as a plateau bounded by highly eroded carbonate rocks, as presented in Figure 3, and clearly shown in the stratigraphic cross-section of the dominant Qurn formation throughout the study area and the related field photos, as displayed in Figure 4.

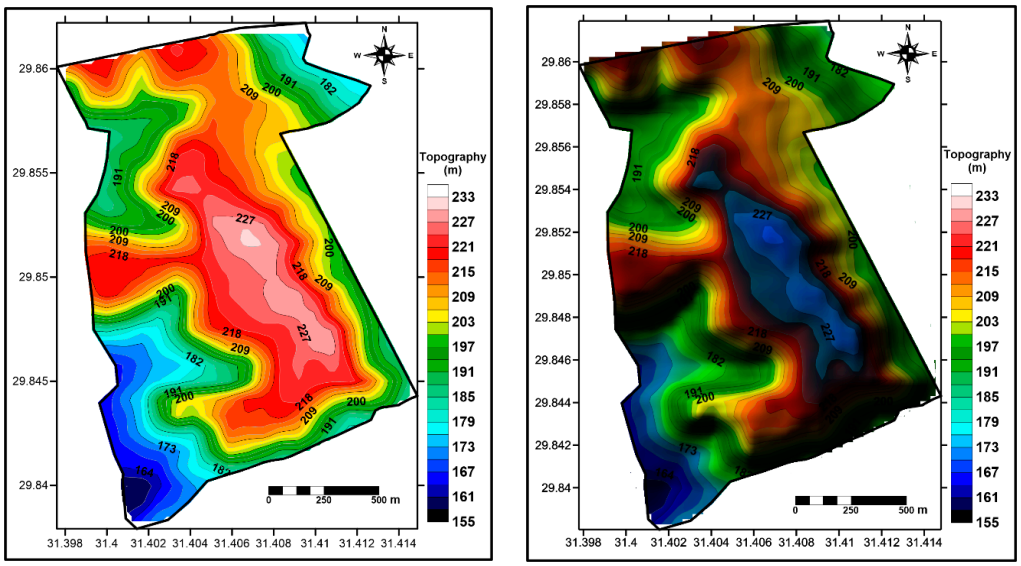


Figure 3. Topography of the study area: (**a**) 2D sheet and (**b**) 3D sheet.

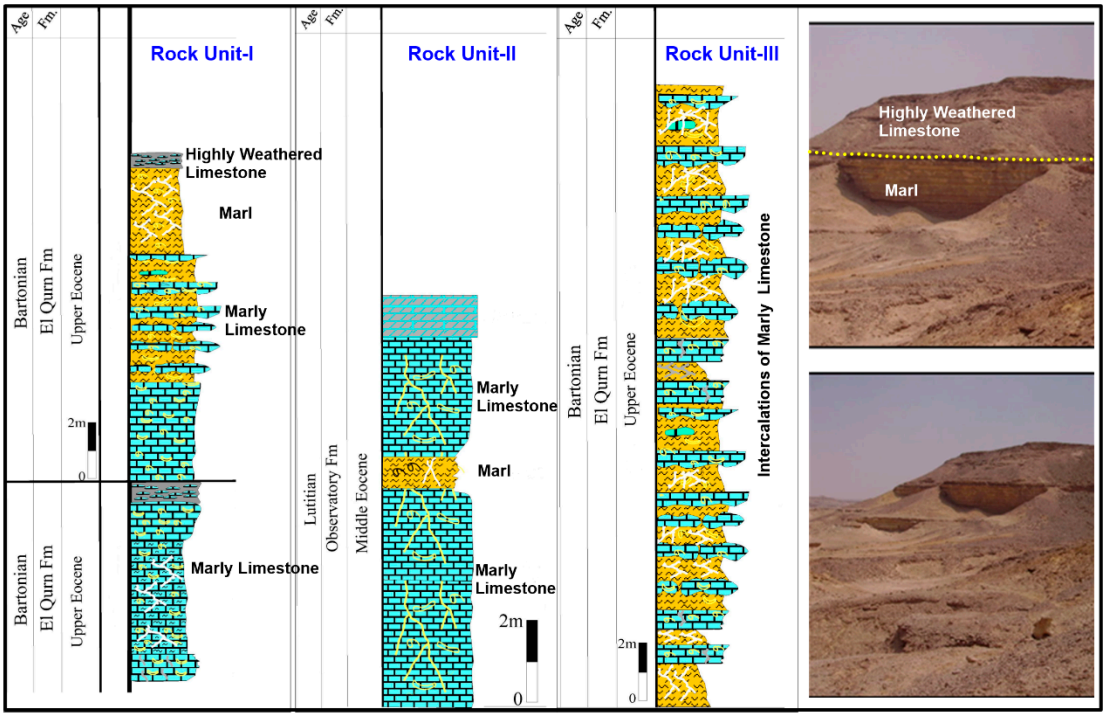


Figure 4. Stratigraphic cross-section of Qurn formation and the related field photos.

This study was prepared to emphasize the importance of properties of soils that are common to both geotechnical (local) and urban planning (regional) studies. There are several types of physical properties and analyses (in the laboratory and in the field) used to evaluate the soil structure and related materials buried in the soil [14–21]. The main objective of the current research is to assess and evaluate the importance of applying surface geophysical techniques for preparing the future land-use plan to verify the sustainability of the new installed urban communities to minimize and avoid the associated hazards and risks of subsurface structural elements and cavities, if present.

2. Materials and Methods

Environmental geophysical surveys (seismic refraction, ground penetrating radar, and geoelectric DC resistivity methods) were carried out to evaluate the subsurface lithological sequence of the extension of Helwan city for preparing the optimal land-use plan. The primary goal of the current study is to demonstrate the capabilities of the utilized geophysical methods for defining the near-surface rocks at the site under investigation and avoid the most unsuitable areas for construction purposes, by applying the systematic methodology through the shown flowchart in Figure 5.

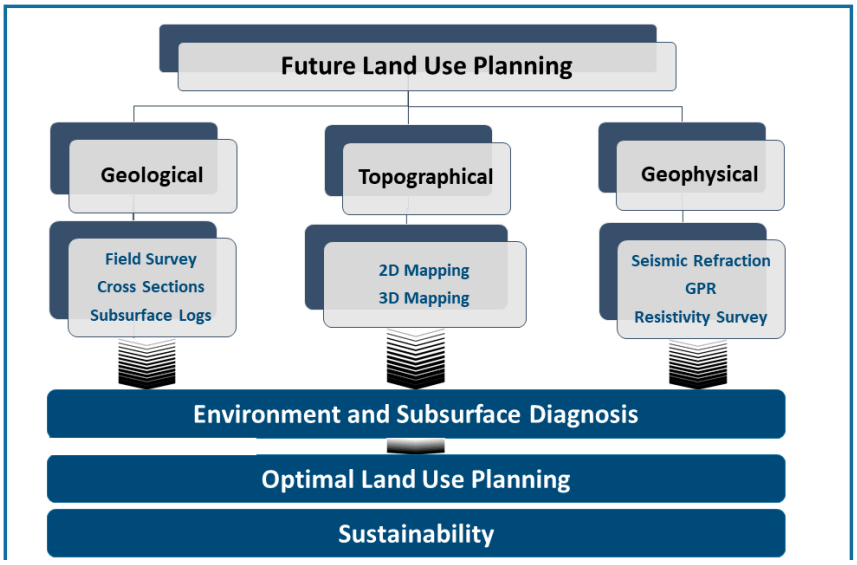


Figure 5. Applied methodology for preparing the land-use plan of the investigated site.

2.1. Seismic Refraction

The geophysical technique of seismic refraction is often conducted as a reconnaissance method in virgin areas. It is most useful where there is at least one high-seismic-velocity bed, having geological interest which extends without significant change over a wide area [22]. In addition, it has been extensively used in environmental, engineering, and hydrogeologic applications, due to the new developments in acquisition instrumentation, sources of sound waves, and updated interpretational computing techniques, which make data collection for site assessment and modeling investigations using seismic refraction methods more efficient and more applicable [23–26].

The method of seismic refraction depends on registering the trip time of the first arrivals for the refracted sound waves up to the ground surface by the inserted geophones on the ground surface and plotting them with the distances between the geophones to investigate the variation in seismic velocities for subsurface rocks with depth [23].

In the present study, the main target for applying seismic refraction techniques is to delineate the site bedrock to determine the overburden thickness, which is essentially important in planning urbanization projects in the extension of Helwan city. The seismic field work was summarized by a total of 20 forward-split-reverse shootings, distributed all over the study area as shown in Figure 6, to perform and anatomize the areal extent of the compressional seismic wave velocity of the bedrock.

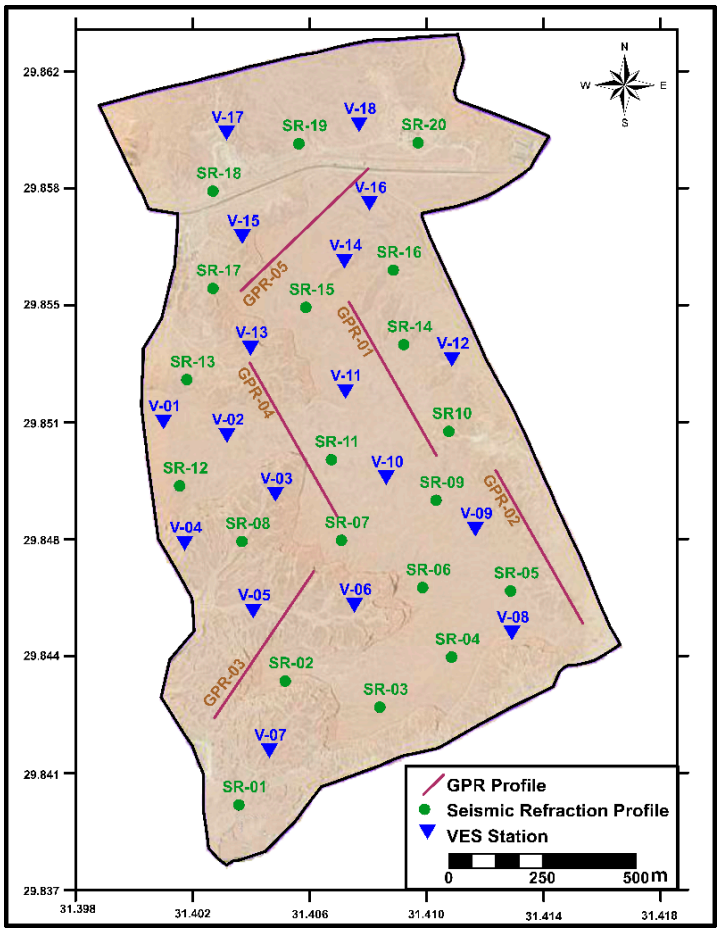


Figure 6. Location map of the conducted geophysical survey in the investigated site.

In order to generate compressional (P) waves, a sledgehammer is utilized to vertically hammer a steel plate on the ground surface. Vertically oriented geophones are used to pick up the ground motion due to generated seismic pulses. A 12-channel digital signal-enhancement seismograph (Strata-Vision-Geometrics) is used in recoding the generated seismic signals. It is known that the quality of seismic data depends on several parameters: the instrument used, topographic variations, geophone location, situation and location of the seismic source, and the surrounding noise. In the present study, the good manner of the collected seismic data is due to the location of the study area away from sources of noise such as surrounding traffic activities, machinery, human activities, and related parameters which greatly reduce the signal-to-noise rate.

2.2. Ground Penetrating Radar

GPR utilizes signals of electromagnetic energy (waves of radio) and the frequencies of the applied GPR technique are always varying from 10 to 1000 MHz, which are transmitted into the earth via a sending antenna placed on the surface of the ground, and simultaneously the receiving antenna picks the reflected up electromagnetic waves to the surface of the ground. When the transmitted signal encounters a subsurface reflector there exists a contrast in the electromagnetic impedance [27–30].

In the current study, a total of five GPR profiles with total lengths of 2700 m were recorded in the investigated site to define the shallow Quaternary deposits and to characterize the potential of subsurface cavities and structural elements (if present), as shown in Figure 6. All GPR sections were recorded by a radar reflection profiling survey method using RAMAC2/MALA Geosciences, and by utilizing 100 MHz unshielded antennas. Then, the measurements were triggered at constant spacings by an odometer wheel.

Most of the GPR surveying was conducted for picking shallow surface exploration and executed in a fixed common offset (reflection profiling configuration). In the current study, this mode was applied by fixing the distance between antennas on the earth's surface and moving on by constant distance along the surveyed lines to image the subsurface targets or reflectors with varying electromagnetic impedance through the conducted GPR traverses, thereby providing continuous GPR records [31,32].

2.3. Geoelectric Resistivity Survey

The main concepts of the geoelectrical sounding resistivity technique are disputed by several researchers. In resistivity surveys, a low-frequency or direct electric current is inserted through the earth by pair of current electrodes. The probable difference in potential is recorded among another pair of electrodes, where the four electrodes are inserted according to the widely applicable Schlumberger configuration, which can be used easily to calculate the corresponding resistivity values [33–36].

The essential objective of sounding resistivity is to identify the vertical change in electric resistivity and/or conductivity with the penetrable depth. Generally, the vertical variation in resistivity with depth must be associated with lateral variations, especially in prevailing nearly horizontal sedimentary deposits. The vertical electrical sounding technique is considered the most applicable geophysical technique for groundwater exploration in many areas around the world [37].

The geoelectrical resistivity survey was conducted by a total of 18 soundings throughout the study area, as illustrated in Figure 6, by utilizing the resistivity meter of SYSCAL-R2. The half spacing of the recording electrodes (potential) was enlarged in a discrete procedure, varying from 0.2 to 10 m to record the contrast in the difference in the potential. The injected electrodes of the current were designed by a half spacing (1 to 100 m) to pick the geological features and the targeted litho-stratigraphic deposits.

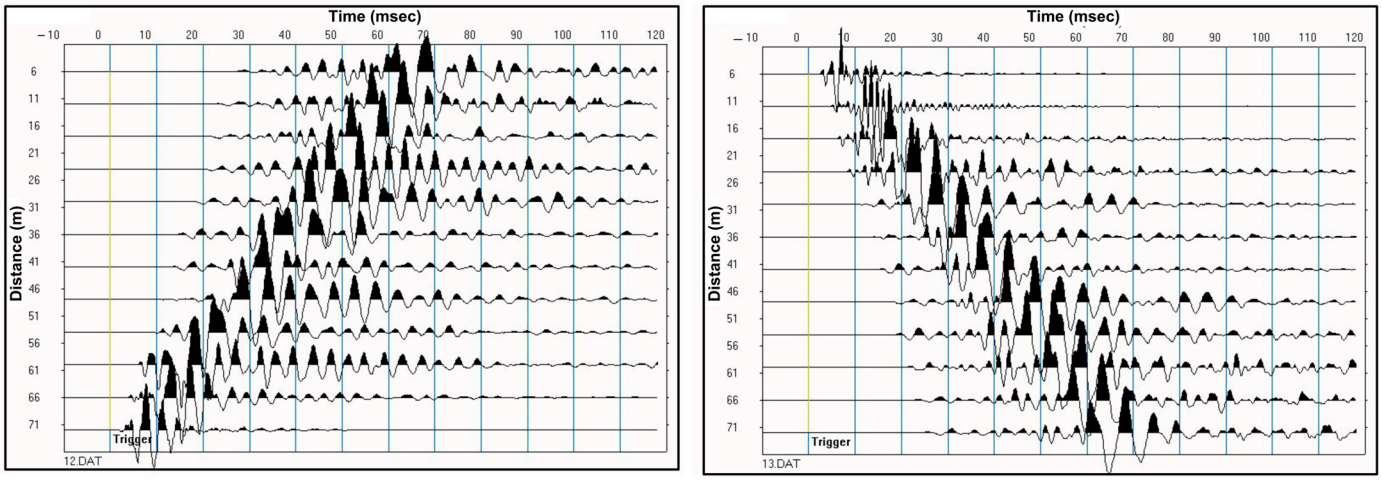
3. Results

The current study is based on the integration and merging of the findings of the applied geophysical techniques (seismic refraction, ground penetrating radar, and geoelectric DC resistivity methods). The following sections briefly describe the concluded results in imaging the shallow subsurface model and determining the most suitable areas for construction purposes.

3.1. Seismic Refraction

Through the current study, a seismic refraction survey was principally applied to delineate subsurface layering, and the bedrock in particular, to evaluate the extension of Helwan city for engineering projects and other inter-related development projects. A sum of twenty profiles of seismic refraction were conducted in the investigated site, with a maximum length of profiles reaching 75 m, the used inter-geophone spacing ranging from 1.5 to 2 m, and the shot-to-first-geophone-spacing was 1.5 m, as presented in Figure 7.

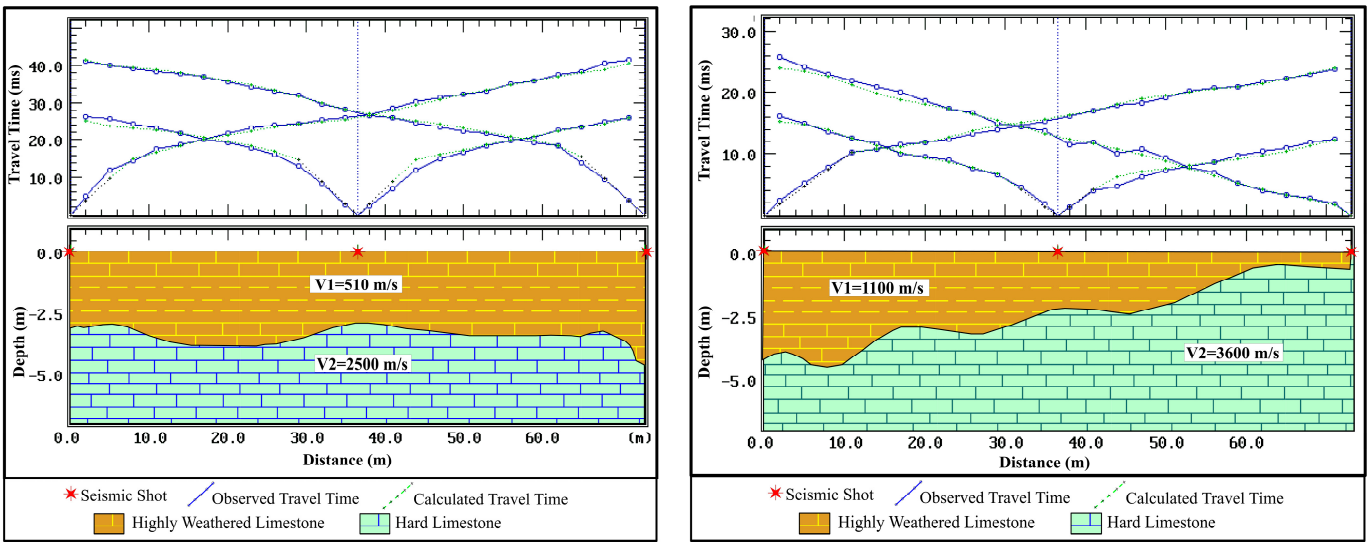
After picking the first arrivals for the conducted records, the evaluation of the collected seismic refraction travel time data was achieved by applying a refraction analysis program "Seis REFA", OYO GEOSPACE [38]. The analysis routine begun with irregularity, reciprocity, and parallelism checks. Velocity–depth models were then calculated using the Ray tracing technique. The calculated parameters (i.e., depth and velocity) are represented in two forms: (1) two-dimensional (2-D) depth–velocity models, which display both vertical and lateral variations in each detected stratum along the profiles; and (2) velocity and depth or thickness contour maps to illustrate the horizontal variation in these parameters through the investigated site.



(**a**) (**b**)

Figure 7. Samples of collected seismic refraction records of the profile SR#11: (**a**) forward shooting and (**b**) reverse shooting.

The calculated velocity–depth models for the conducted seismic refraction profiles can be described by two main seismic layers: (1) thin surface layer with low seismic velocity in the range of 400–1100 m/s, which corresponds to highly weathered limestone, with an average thickness of 3 m; and (2) a bottom stratum with higher seismic velocity of in the range of 2100–3600 m/s, which corresponds to the bedrock that is composed of hard limestone that extends to the maximum penetrable depth, as shown in Figure 8.

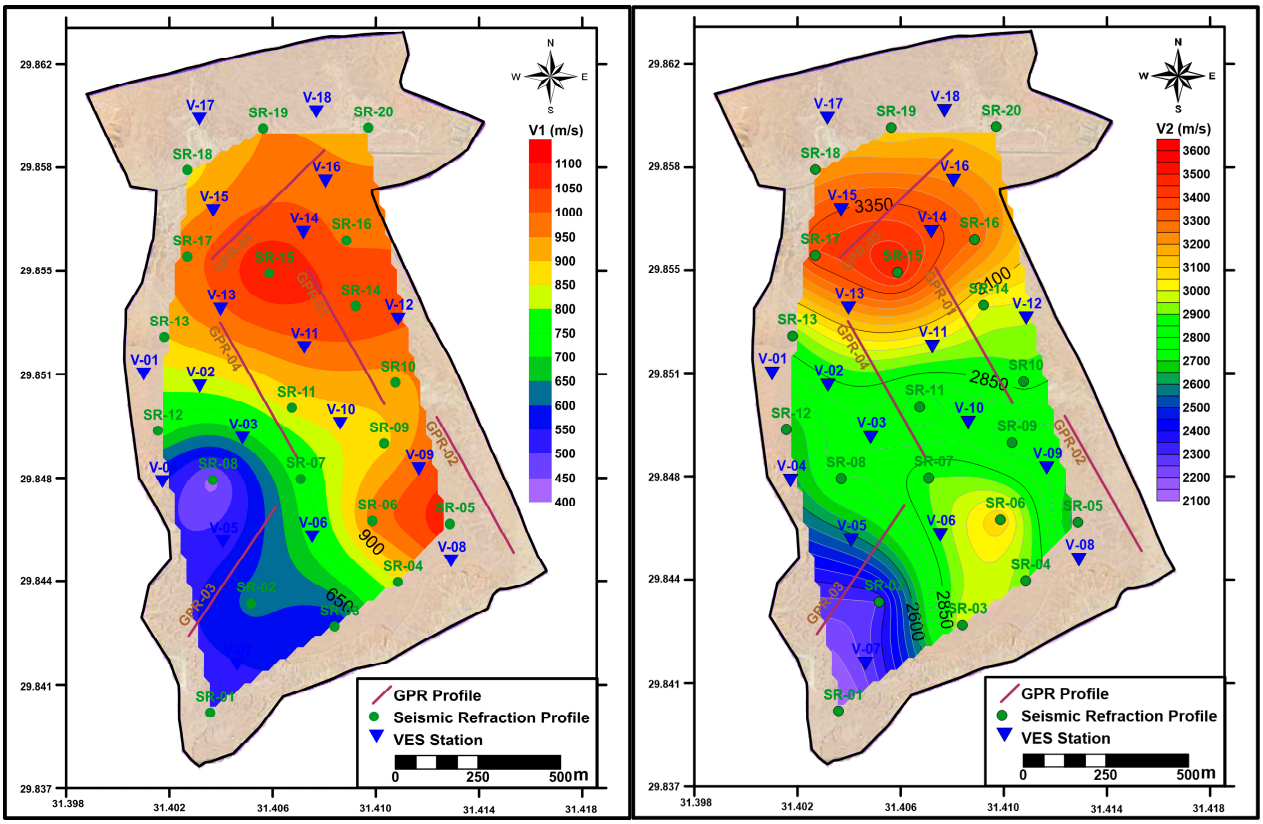


(**a**) (**b**)

Figure 8. Travel time curves and calculated velocity–depth model of seismic refraction profiles that describe in its upper part both observed and calculated travel time curves and on its lower part the calculated depth–velocity model. The good agreement between the observed and calculated travel times indicates the integrity of the calculated depth–velocity models of the profiles (**a**) SR#1 and (**b**) SR#15.

The areal distribution of seismic velocity throughout the study area was formalized by constructing two contour maps, which reflect that the seismic velocity of the first layer ranges between 900–1000 m/s for most of the investigated site while the southwestern part is characterized by low seismic velocity (400–350 m/s), as shown in Figure 9a. The

seismic velocity of the second strata is also characterized by low seismic velocity only at the southwestern parts of the investigated site, as indicated in Figure 9b.



(**a**) (**b**)

Figure 9. Seismic velocity contour map of (**a**) surface layer and (**b**) second layer.

3.2. Ground Penetrating Radar

Interpretation of radar data concluded the ordered procedure: reduction, correction, and filtering of the acquired raw data; distinguishing the reflections and associated noise; identification of velocity; recording two-way travel times of reflected events; conversion of reflection times to depths; and integration of the gathered data from the marked lines to image the nature and main reasons of the reflection criteria through the conducted GPR traverses.

From the standard tabular values of EM velocity for limestone deposits of 0.15–0.11 m/ns, the maximum penetrable depth reached nearly 15 m, and the generic subsurface model can be described as the following: surface highly weathered limestone of a thickness averaged of 0.7 m, underlain by fractured marly limestone sediments of a thickness averaged of 4.4 m, and a second layer of hard limestone that extended the maximum penetrable depth of the GPR sections, as indicated in Figure 10.

3.3. Geoelectric Resistivity Survey

A total of 18 vertical electrical soundings (VES) were surveyed at the investigated site, as displayed in Figure 6, utilizing an electrode arrangement named Schlumberger with an extreme half electrode distance (AB/2) reaching 100 m. A digital, signal-enhancement resistivity meter (SYSCAL-R2) was utilized to collect the field data of the resistivity survey. The resistivity data were measured every sixth of a logarithmic decade to ensure a detailed investigation and interpretation accuracy.

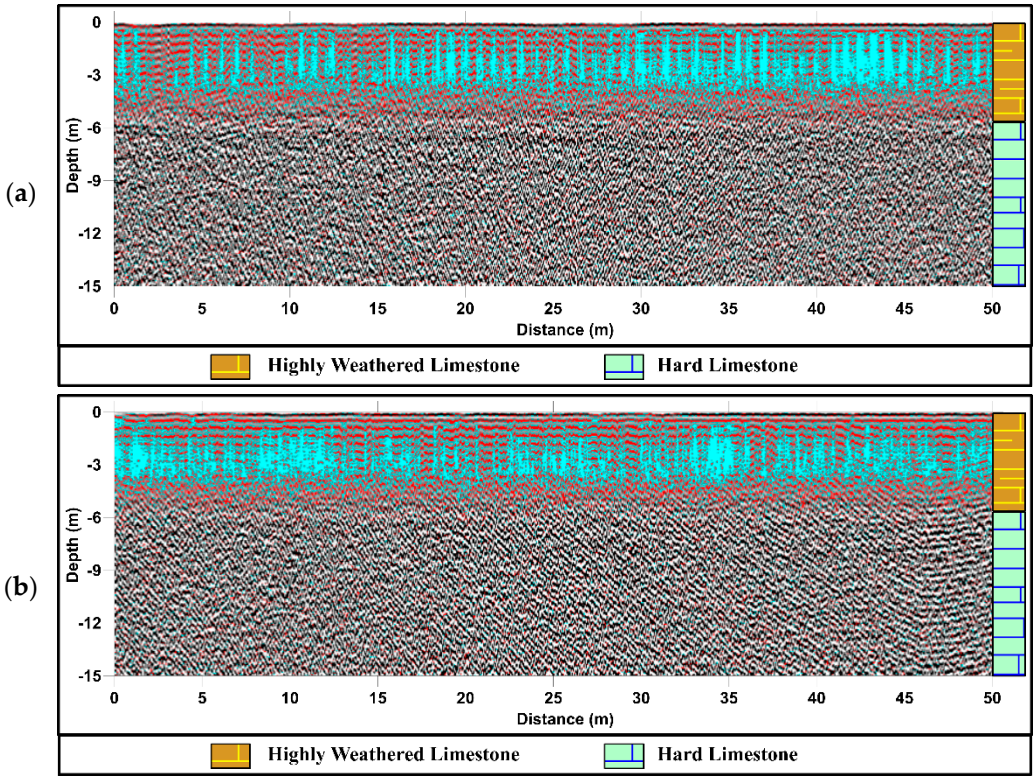


Figure 10. Samples of GPR records: (**a**) GPR-01 and (**b**) GPR-02.

Investigating the behavior of the gathered plotted curves of resistivity data introduce a preliminary impression of the apparent resistivity distribution through the investigated site, which displayed two types of QH and KH resistivity curves through the investigated site and considered a straight reference on the approximate resistivity homogeneity through the study area, as shown in Figure 11.

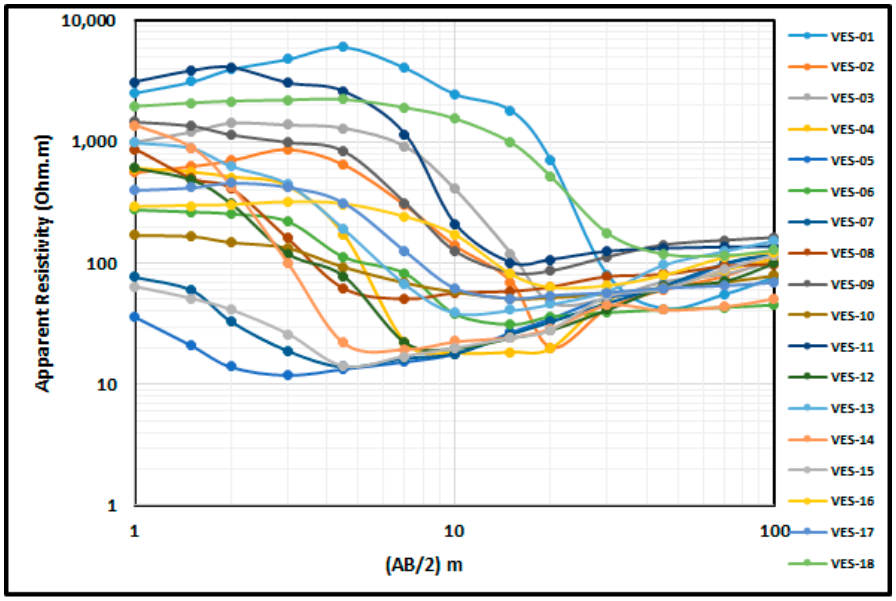
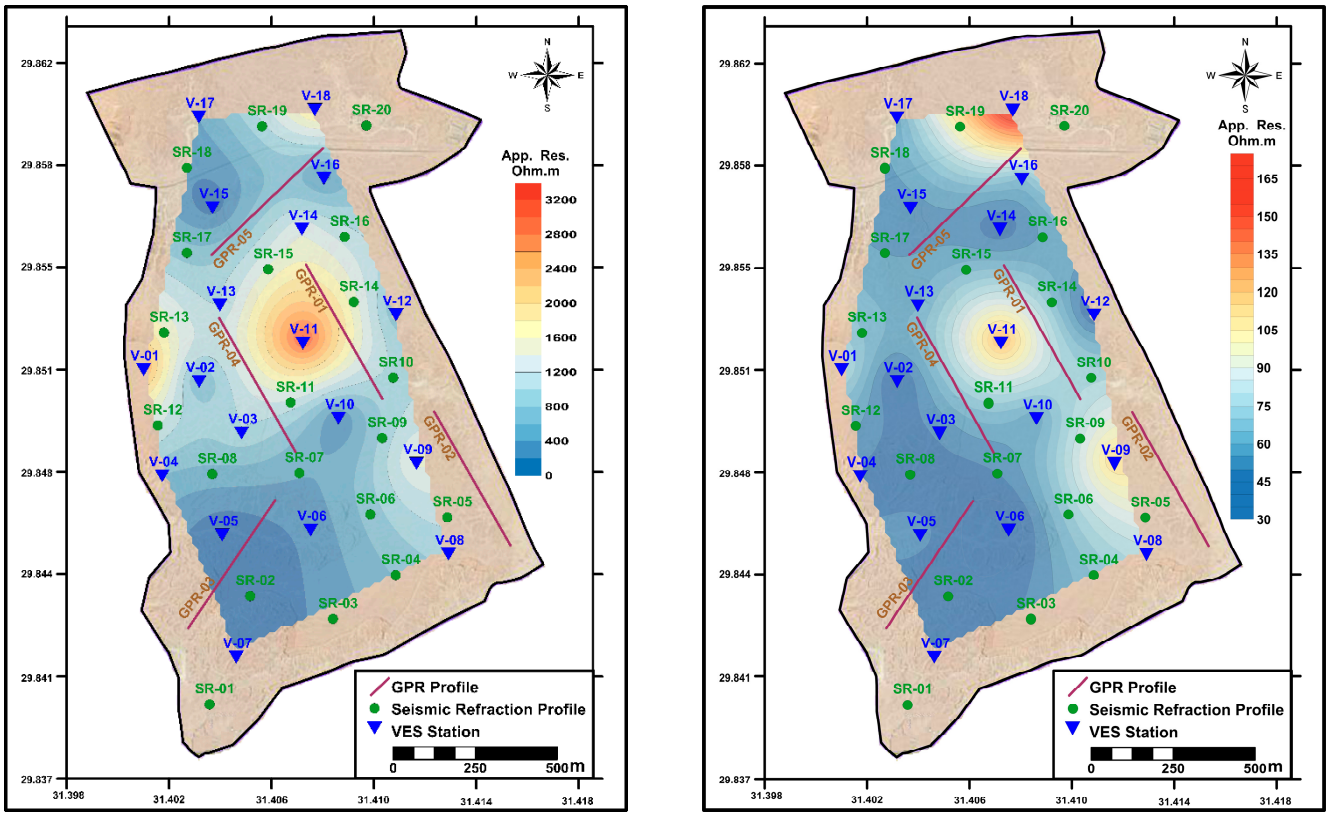


Figure 11. Acquired vertical electrical soundings throughout the study area.

Two contour maps of apparent resistivity at electrode spacings (AB/2) equal to 1 and 30 m were constructed for analyzing the areal distribution of apparent resistivity at different levels, which can perform a preliminary impression of the apparent resistivity at

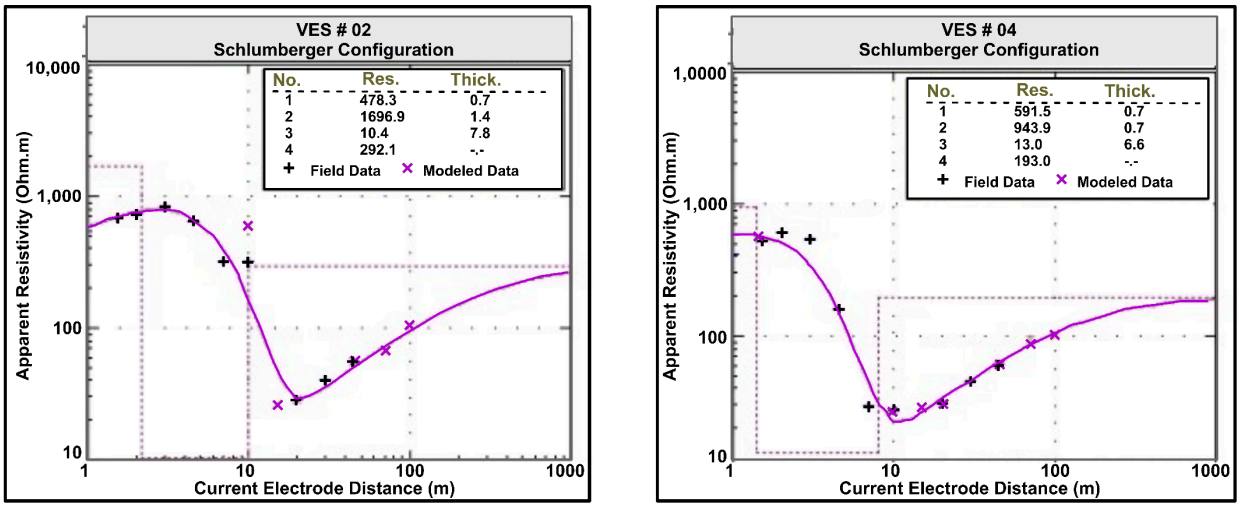
the picked level according to the selected electrode spacing, as shown in Figure 12. The apparent resistivity values at the spacing (1 and 70 m) introduces the same distribution of apparent resistivity throughout the study area, which was characterized by the low range at the southwestern sector of the investigated area.



(**a**) (**b**)

Figure 12. Apparent resistivity contour maps: (**a**) AB/2 = 1 m and (**b**) AB/2 = 30 m.

Quantitatively, the gathered geoelectrical resistivity data were interpreted in two parallel procedures: (1) a primary model of resistivity was generated based upon the Master Curves approach, and (2) the primary model was entered into a software iterative package to model and calculate the final earth resistivity sounding. Firstly, a preliminary model is assumed for each geoelectric resistivity sounding curve utilizing the approach of Master Curves [39] and the geological background. The resulting initial model is composed of true resistivity and thickness values. Secondly, the approach of computerized iteration is applied to define the primary attained model as considered in the starting step. The software iterative package "Resist" [40] is executed to optimize the final model of resistivity. The justification of the calculated end resistivity model is governed by computing the Root Mean Square Error (RMS Error) among the observed and computed resistivity values, which has a range between 1.7–6.3%, as presented in Figure 13.



(**a**) (**b**)

Figure 13. Samples of final interpreted models of the conducted VESs for (**a**) VES-02 and (**b**) VES-04.

The common subsurface geoelectrical resistivity model of the investigated site can be represented by two main distinctive resistivity layers: (1) a surface overburden layer with true resistivity values ranging between 397.7–6039.2 Ohm.m. which corresponds to the surface fractured dry weathered sediments, with an average thickness of about 0.5 m, which was not represented at all the conducted VESs and was underlaid by argillaceous limestone with resistivities of 4.3–61.6 Ohm.m with an average thickness of nearly 4.8 m; and (2) a second layer with a true resistivity exceeding 190 Ohm.m equivalent to the bedrock of the investigated site, as shown in Figure 13.

To anatomize the variation in the computed parameters of the geoelectrical resistivity model (thickness and true resistivity) in the perpendicular level through the investigated site, three cross-sections of geoelectric resistivity were implemented in the vertical and horizontal planes of the investigated site, where the perpendicular scale is equivalent to the corresponding elevation with respect to the sea level and the plotted horizontal axis represents the horizontal offsets among the surveyed soundings throughout the length of the section. The geoelectric resistivity cross-sections concluded the following: the profiles P1 and P2 run from north to south, while P2 runs east to west, and all the profiles show the overburden deposits fluctuating between weathered deposits (370–953 Ohm.m) and argillaceous limestone (10–61.6 Ohm.m) ending by the bed rock of highly compacted limestone (more than 190 Ohm.m), as shown in Figure 14.

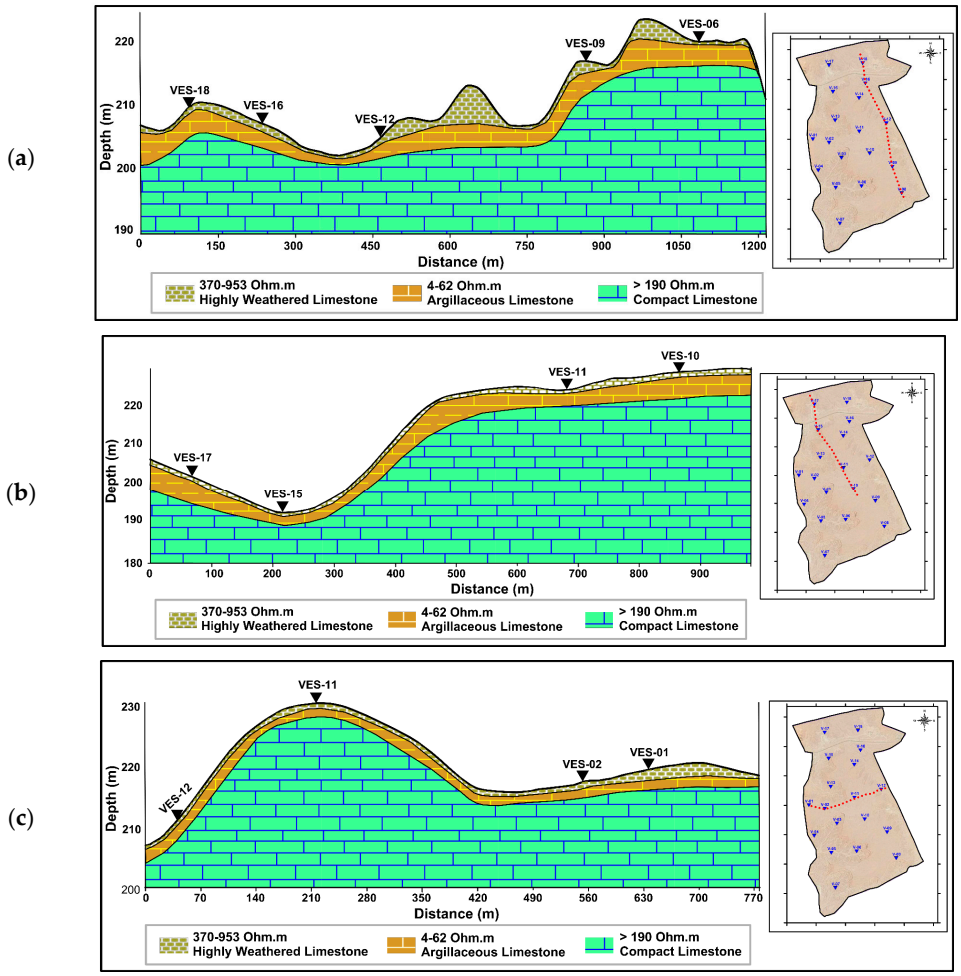


Figure 14. Geoelectric resistivity cross-sections: (**a**) profile-01, (**b**) profile-02, and (**c**) profile-03.

4. Discussion

Reasonable integration of different geophysical and geological data can be utilized intensively to evaluate the physical characteristics and properties of the subsurface layering sequence and to determine the structural elements that can be utilized for optimal planning of the future land-use of the investigated site [41].

Geologically, a field survey accomplished with q literature survey [13,42,43] at many geological outcrops and points of inspection reveals the investigated site represented by main geological units related to various geological formations. The dominant formation in the investigated site is the formation of Qurn, which is composed of main two geological units representing most of the investigated site, which corresponds to the clayey marl that represents the main geotechnical problem.

Interpretation of surveyed seismic refraction profiles, as supported and confirmed by GPR results, subdivided the near-surface subsurface deposits into main two layers: the first layer, equivalent to highly weathered limestone which is matched with geological inspection points and the obtained results of the resistivity sounding data, and a second layer of hard limestone. In addition, the geoelectrical resistivity data (VES), utilizing the Schlumberger configuration, point out the investigated site represented by different geologic units as stated by the ranges of resistivity values, indicating that the subsurface stratigraphic section consists of two main distinctive layers of overburden deposits fluctuating between weathered deposits and argillaceous limestone ending by bed rock of highly compacted limestone.

Based on the findings and the obtained results of the merged and integrated environmental geological and geophysical techniques, it has been possible to divide the study area

into two main units with distinct geophysical and geological characteristics, which can be described briefly as the following: unit (A) that covers most portions of the investigated site except the southwestern part and represents the relatively optimum area for construction purposes after removing the overburden deposits (highly weathered and argillaceous limestone deposits), which can used for heavy construction activities; and unit (B) that covers the southwestern part of the investigated site, which is highly weathered and marked by low seismic velocities and low true resistivity values, in addition to that it can be described as very steep lowland and can be used for open areas such as parking and gardens, as illustrated in Figure 15.

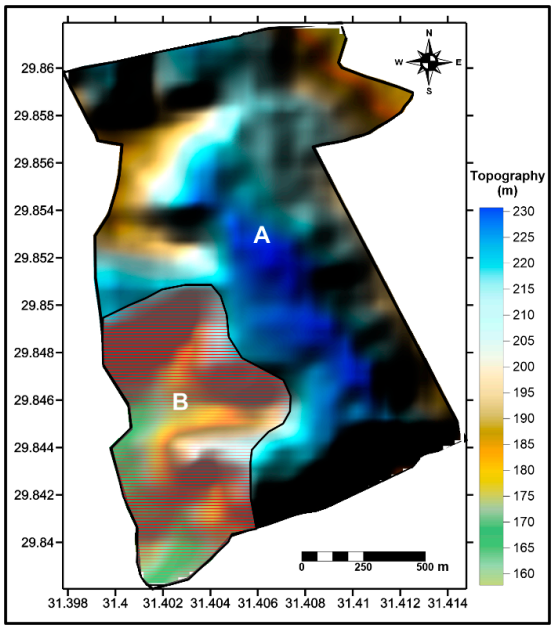


Figure 15. Suggested land-use map of the investigated site: A unit, that represent the optimum area for construction purposes, and B unit, that equivalent to open, parking, garden areas.

5. Conclusions

The fundamental target of the current research involves the use of integrated geological and near-surface geophysical techniques to optimize the land-use plan for construction purposes and avoid the high-risk areas in the extension of Helwan city, Egypt. The applied geophysical techniques were utilized for monitoring the variations in subsurface distribution of geoelectrical and seismic velocity heterogeneities, in addition to the GPR signatures. The findings concluded that the subsurface sequence of the investigated site is represented mainly by two main layers: the first layer that is equivalent to highly weathered and argillaceous limestone, and the second layer that is corresponding to bedrock of limestone.

The optimal land-use map was generated for the concerned study area by merging the integrated results of applied geological and geophysical techniques to determine the most suitable areas for construction purposes and avoid the high potential of risk areas. The investigated site was branched to two main units by avoiding the highly weathered, low seismic velocities and low true resistivity values, which also can be described as very steep lowland in southwestern part of the study area.

Finally, the current study encourages to utilize and apply the specifically designed integrated geological and geophysical techniques of seismic refraction, geoelectrical resistivity sounding, and GPR for obtaining a reasonable subsurface image, which can perform the optimal geotechnical investigative program for the study area and its surroundings to maintain the sustainability of the future urban communities.

It is so important and vital to understand the subsurface geological conditions of the new planned areas for constructional projects to prepare a sustainable land-use plan for

the investigated site. Therefore, the application, integration, and merging of a quantitative geological and geophysical survey program prior to the design and planning of the new urban communities, as applied through the current study, will provide a clear subsurface image and minimize the related costs of the geotechnical boring studies. Finally, the presented approach through the current study can be applied to more general situations.

Funding: The author would like to thank the Deanship of Scientific Research at Umm Al-Qura University for supporting this work by Grant Code: 22UQU4330935DSR02.

Institutional Review Board Statement: Not applicable.

Informed Consent Statement: Not applicable.

Data Availability Statement: The data used to support the findings of this study are available from the corresponding author upon request.

Conflicts of Interest: The authors declare no conflict of interest.

References

1. Thacker, S.; Adshead, D.; Fay, M.; Hallegatte, S.; Harvey, M.; Meller, H.; O'Regan, N.; Rozenberg, J.; Watkins, G.; Hall, J.W. Infrastructure for sustainable development. *Nat. Sustain.* **2019**, *2*, 324–331. [CrossRef]
2. Lesko, K.T. The Deep Underground Science and Engineering Laboratory at Homestake. *AIP Conf. Proc.* **2009**, *1182*, 230.
3. Feng, X.T.; Wu, S.Y.; Li, S.J.; Qiu, S.L.; Xiao, Y.X.; Feng, G.L.; Shen, M.B.; Zeng, X.H. Comprehensive field monitoring of deep tunnels at Jinping underground laboratory (CJPL–II) in China. *Chin. J. Rock Mech. Eng.* **2016**, *35*, 649–657. (In Chinese with English Abstract)
4. Shang, Y.-J.; Yang, C.-G.; Jin, W.-J.; Chen, Y.-W.; Hasan, M.; Wang, Y.; Li, K.; Lin, D.-M.; Zhou, M. Application of Integrated Geophysical Methods for Site Suitability of Research Infrastructures (RIs) in China. *Appl. Sci.* **2021**, *11*, 8666. [CrossRef]
5. McCann, D.M.; Culshaw, M.G.; Fenning, P.J. Setting the standard for geophysical surveys in site investigation. *Geol. Soc. Lond. Eng. Geol. Spec. Publ.* **1997**, *12*, 3–34. [CrossRef]
6. El-Megharbel, N. Sustainable Development Strategy: Egypt's Vision 2030 and Planning Reform, Integrated Approaches to Sustainable Development Planning and Implementation. 2015. Available online: http://mop.gov.eg/Vision/EgyptVision.aspx (accessed on 10 October 2022).
7. Ali, H.; Abdel-Latif, A.; Magdy, D.; El-Sharkawy, K.; William, M.; Magid, M. *Egypt SDS 2030: Between Expectations and Challenges to Implement*; The American University in Cairo, The School of Global Affairs and Public Policy: New Cairo, Egypt, 2018.
8. Robaa, S.M. Some aspects of the urban climates of Greater Cairo Region, Egypt. *Int. J. Clim.* **2013**, *33*, 3206–3216. [CrossRef]
9. Robaa, S.M.; Hafez, Y.Y. Monitoring Urbanization Growth in Cairo City. *J. Eng. Appl. Sci.* **2002**, *49*, 667–679.
10. Robaa, S.M. Impact of Urbanization on Meteorology and Human Comfort in Greater Cairo, Egypt. Ph.D. Thesis, Cairo University, Cairo, Egypt, 1999.
11. Said, R. Explanatory Notes to Accompany the Geological Map of Egypt. *Geol. Surv. Egypt* **1971**, *3*, 89–105.
12. Strougo, A. The Middle-Eocene-Upper-Eocene boundary in Egypt. *Ann. Geol. Surv. Egypt* **1979**, *9*, 454–469.
13. Moustafa, A.R.; Yehia, M.A.; Abdel-Tawab, S. Structural Setting of the Area east of Cairo, Maadi, and Helwan. *Middle East Res. Cent. Ain Shams Univ. Sc. Res. Ser.* **1985**, *5*, 40–64.
14. Korkmaz, B.; Ozcep, F. Fast and Efficient Use of Geophysical and Geotechnical Data in Urban Microzonation Studies at Small Scales: Using Sisli 669 (Istanbul) As Example. *Int. J. Phys. Sci.* **2010**, *5*, 158–169.
15. Özçep, F.; Boyraz, G.; Tezel, O.; Alp, H.; Alpaslan, N.; Karabulut, S. Geophysical and Geotechnical Factors in Urban Planning: Bursa (Nilufer, Osmangazi, and Yildrim) Cases. *Nat. Hazards Earth Syst. Sci. Discuss.* **2020**. *preprint*. [CrossRef]
16. Ozcep, F.; Ozcep, T. Geophysical Analysis of the Soils for Civil (Geotechnical) Engineering and Urban Planning Purposes: Some Case Histories from Turkey. *Int. J. Phys. Sci.* **2011**, *6*, 1169–1195. [CrossRef]
17. Alpaslan, N.; Özçep, F. Arkeolojik Aramalarda ve Geoteknik Arastırmalarda Zemin/Toprak Özelliklerinin Önemi. In Proceedings of the Symposium on Geophysics and Remote Sensing in Determination of Near-Surface Structures (GARS 2008), Izmir, Turkey, 30 April–2 May 2008; pp. 201–204.
18. Ozcep, F.; Tezel, O.; Asci, M. Correlation Between Electrical Resistivity and Soil-Water Content: Istanbul and Golcuk. *Int. J. Phys. Sci.* **2009**, *4*, 362–365.
19. Ozcep, F.; Guzel, M.; Kepekci, D.; Laman, M.; Bozdag, S.; Cetin, H.; Akat, A. Geotechnical and Geophysical Studies for Wind Energy Systems in Earthquake-prone Areas: Bahce (Osmaniye, Turkey) case. *Int. J. Phys. Sci.* **2009**, *4*, 555–561.
20. Ozcep, T.; Ozcep, F.; Ozel, O. Comparison between Vs30 and Site Amplifications, and Their Reliability for Seismic Design Codes: Adapazari (Turkey) Case. In Proceedings of the WCCE-ECCE-TCCE Joint Conference—Earthquake and Tsunami: Civil Engineering Disaster Mitigation Activities Implementing Millennium Development Goals, Istanbul, Turkey, 22–24 June 2009.
21. Karabulut, S.; Özel, O.; Ozcep, F. New Method to Determination of Fundamental Frequency of Engineering Structures Against Earthquake Hazard: Microtremor Methods and Case Study. *E-J. New World Sci. Acad.* **2009**, *4*, 428–441.

22. Dobrin, M.B. *Introduction to Geophysical Prospecting*, 3rd ed.; McGraw-Hill Book Co., Inc.: New York, NY, USA, 1976.
23. Haeni, F.P. Application of seismic refraction methods in groundwater modeling studies in New England. *Geophysics* **1986**, *51*, 236–249. [CrossRef]
24. Ugwu, S.A. Determination of depth to bedrock in Afikpo syncline of the Benue Trough, Nigeria, using seismic refraction methods. *Sci. Afr.* **2008**, *7*. [CrossRef]
25. Ayolabi, E.A.; Adeoti, L.; Oshinlaja, N.A.; Adeosun, I.O.; Idowu, O.I. Seismic Refraction and Resistivity Studies of Part of Igbogbo Township, south-west Nigeria. *J. Sci. Res. Dev.* **2009**, *11*, 42–61.
26. Varughese, A.P.; Kumar, N. Seismic Refraction Survey a Reliable Tool for Subsurface Characterisation for Hydropower Projects. In Proceedings of the Indian Geotechnical Conference, Kochi, India, 15–17 December 2011; pp. 137–139.
27. Daniels, D.; Gunton, D.; Scott, H. Introduction to subsurface radar. *IEE Proc. F Commun. Radar Signal Process.* **1988**, *135*, 278–320. [CrossRef]
28. al Hagrey, S.A.; Muller, C. GPR study of pore water content and salinity in sand. *Geophys. Prospect.* **2000**, *48*, 63–85. [CrossRef]
29. Muller, W. Trial of ground penetrating radar to locate defects in timber bridge girders. In Proceedings of the State Conference of the Institute of Public Works Engineering Australia (IPWEA) Queensland Division, Noosa Lakes, Australia, 6–10 October 2002.
30. Greaves, R.J.; Lesmes, D.P.; Lee, J.M.; Toksöz, M.N. Velocity variations and water content estimated from multi-offset, ground-penetrating radar. *Geophysics* **1996**, *61*, 683–695. [CrossRef]
31. Baker, G.S.; Jordan, T.E.; Talley, J. An Introduction to Ground Penetrating Radar (GPR). In *Stratigraphic Analyses Using GPR*; Baker, G.S., Jol, H.M., Eds.; Geological Society of America Special Paper 432; Geological Society of America: Boulder, CO, USA, 2007; pp. 1–18. [CrossRef]
32. Balanis, C.A. *Antenna Theory, Analysis, and Design*; John Wiley & Sons: New York, NY, USA, 1997; p. 941.
33. Zohdy, A.A.R.; Eaton, G.P.; Mabey, D.R. *Application of Surface Geophysics to Ground Water Investigations*; USGS Numbered Series; USGS: Reston, VA, USA, 1974; Volume 116. [CrossRef]
34. Parasnis, D.S. *Applied Geophysics*, 3rd ed.; Chapman and Hall: London, UK, 1979; Volume 269.
35. Mousa, D.A. The role of 1-D Sounding and 2-D Resistivity Inversions in Delineating the Near Surface Lithologic Variations in Tushka area, south of Egypt. *Geophys. Soc. J.* **2003**, *1*, 57–64.
36. Omoyoloye, N.A.; Oladapo, M.I.; Adeoye, O.O. Engineering Geophysical Study of Adagbakuja Newtown Development South-western Nigeria. *J. Earth Sci.* **2008**, *2*, 55–63. Available online: https://medwelljournals.com/abstract/?doi=ojesci.2008.55.63 (accessed on 10 October 2022).
37. Parasnis, D.S. *Principles of Applied Geophysics*, 4th ed.; Chapman and Hall: London, UK, 1986; pp. 371–373, 137–150.
38. OYO, Geospace. *SeisREFRA. Refraction Analysis Program*; Oyo Geospace Corporation: Houston, TX, USA, 1991.
39. Orellana, E.; Mooney, H.M. *Master Tables and Curves of Vertical Electrical Sounding over Layered Structures*; Intersciencia: Madrid, Spain, 1966; p. 150.
40. Van Der Valpen, B.P.A. Resist, Version 1.0, a Package for the Processing of the Resistivity Sounding Data. Master's Thesis, ITC, Delft, The Netherlands, 1988.
41. Rodríguez, A.I.; Ocaña, R.E.; Flores, D.; Martinez, P.; Casas, A. Environment diagnosis for land-use planning based on a tectonic and multidimensional methodology. *Sci. Total Environ.* **2021**, *800*, 149514. [CrossRef]
42. Atya, M.; Khachay, O.A.; Soliman, M.; Khachay, O.Y.; Khalil, A.; Gaballah, M.; Shaaban, F.; El-Hemali, I. CSEM Imaging of the Near Surface Dynamics and its Impact for Foundation Stability at Quarter 27, 15th of May City, Helwan, Egypt. *Earth Sci. Res. J.* **2010**, *14*, 76–87.
43. Farag, I.; Ismail, M. Contribution to the stratigraphy of the Wadi Hof Area (northeast Helwan). *Bull. Fac. Sci. Cairo Univ.* **1959**, *34*, 147–168.

Disclaimer/Publisher's Note: The statements, opinions and data contained in all publications are solely those of the individual author(s) and contributor(s) and not of MDPI and/or the editor(s). MDPI and/or the editor(s) disclaim responsibility for any injury to people or property resulting from any ideas, methods, instructions or products referred to in the content.